

# Correlation characteristics of laser-induced soot incandescence and flame luminosity in diesel spray combustion

Montanaro, A.\*<sup>1</sup>, Allocca, L.<sup>1</sup>, Zhang, A.<sup>2</sup>, Lee, S.-Y.<sup>2</sup>

<sup>1</sup> Istituto Motori – CNR, Naples (Italy)

<sup>2</sup> Michigan Tech University, Houghton (USA)

## Abstract

Understanding of soot formation and oxidation processes in diesel spray flame is significantly limited when using laser-based measurement due to its low-frequency operation. With the help of the advanced high-speed camera technology, visualization of flame luminosity in the transient diesel spray combustion is readily realized. While both laser-induced incandescence (LII) and flame luminosity are believed to originate from soot in diesel spray combustion, the correlation of actual planar soot field and volume integrated flame luminosity is unknown. The current work was devoted to quantitatively characterize in detail the possible correlation existing between the laser-induced incandescence (LII) of soot signals and flame luminosity. Diesel spray test was performed using ULSD #2 fuel of different injection pressures spraying into ambient density of 25.4 kg/m<sup>3</sup> under the ambient temperature of 900 K with 15% O<sub>2</sub> environment. Simultaneous measurement of LII and high-speed flame luminosity was conducted. 2D-based and 3D-based image correlations were conducted by applying three-point Abel inversion and volumetric integration, respectively. A weak image correlation was recognized for the two imaging techniques. It was found that the presence of turbulence, acquisition wavelength and soot temperature distribution can affect the correlation results.

## Introduction

Soot formation processes in turbulent spray flames under high pressure and high temperature environment have been studied extensively. Techniques including planar laser-induced incandescence (LII), laser extinction, two-color imaging, and flame luminosity have been widely used to visualize the transient soot formation field [1-10]. Among these techniques, LII has become a common approach for *in-situ* soot field measurement. With the help of laser extinction, quantitative measurements such as soot volume fraction, number density, particle size, and temperature distribution can be achieved [2-4, 6, 8, 9]. In parallel, flame luminosity visualization has been significantly advanced by high-speed imaging system and time-resolved luminosity is available for transient flame [4, 11, 12].

Dec [1] proposed a conceptual model of combusting two-phase fuel jet based on experimental visualization of flame and soot formation. Spray combustion initiates with an auto-ignition of premixed burn near the lift-off location, and rapidly transit to a mixing-controlled quasi-steady mode. High soot concentration forms in the head vortex region of the spray, resulting in a layer of soot inside the diffusion flame. Studies under typical diesel engine conditions show that soot formation characteristic is sensitive to a variety of parameters including ambient density, temperature, injection pressure, nozzle orifice size, ambient oxygen level, and local turbulence level [2, 6, 12]. Significant soot forms at high ambient gas temperature conditions where the flame lift-off length is short. When the flame starts closer to the injector tip, there is usually less time and space for air entrainment and rich fuel-air mixture forms locally, which is directly

related to soot yields [2, 13]. Fuel properties also affect soot formation pattern. Higher oxygenated fuel is more likely to generate soot in the center part of the jet rather than the periphery because of available O atoms in the fuel stream [6]. Efforts have also been made to investigate the evolution of soot field structure within the fuel jet flame. By acquiring temporally-resolved luminosity and LII signals from combusting jet, Cenker et al. [9] were able to observe soot formation starting from the spray periphery and expanding into the core region at a later time.

For most of the observations and findings obtained from laser-based soot measurements of diesel spray combustion, temporally-resolved information of soot field is usually not acquired from a single event. This is a common difficulty for low-frequency, i.e., 10 Hz, operation of laser-based experimental technique. However, due to the fact that spray combustion is highly transient with different scales of turbulence, the shot-to-shot variation in spray combustion could introduce extra challenge on image processing and lead to unjustified conclusions. In contrast, high-speed camera is able to provide a fine time resolution for the transient flame that features time scale of milliseconds.

Similarities exist between the signals obtained from flame luminosity imaging and LII. Flame luminosity results mainly from two sources [11, 12]. Chemiluminescence from radicals such as OH, CH, and other intermediate species emits in the early stage of spray combustion. Magnitude of the chemiluminescence signals is usually low and specific to certain wavelengths, and flame temperature is low. The other source, the incandescence of soot particles, serves as the majority of the flame luminosity. Soot particles are clusters of

---

\* Corresponding author: [a.montanaro@im.cnr.it](mailto:a.montanaro@im.cnr.it)

unburned carbon and form within the diffusion flame where the temperature is relatively high. Incandescence signals are emitted from “hot” soot particles, usually observed as bright, broadband luminosity. Thus, the flame luminosity signal is essentially an indication of soot within the flame region at each time instant. In parallel, LII technique utilizes an external source of energy to heat up all soot particles within the combusting jet. By capturing glowing soot particles from this incident heating, soot field distribution can be visualized. LII intensity is correlated with soot particle volume fraction [14]. It can be seen that both the luminosity and LII signals originate from the same source and a similar distribution at a given time instant can be expected.

In the current study, a combination of LII and flame luminosity imaging techniques was applied to the same spray combustion event. Given a possible correlation existing between the two types of signals, an effort is devoted to correlating the images captured by both techniques on a pixel-to-pixel base. To the authors’ knowledge, this is the first attempt of quantitative image analysis on diesel spray combustion. It is expected that a positive correlation can help to extend the instantaneous LII information to a longer time span for the turbulent combustion event.

### Experimental setup

Ambient conditions similar to those inside a diesel engine chamber were simulated in a constant volume combustion vessel. A single axial nozzle solenoid high-pressure diesel injector was mounted to one side port of the vessel. The injector has a converged nozzle with 1.5 k-factor. A pre-burn procedure has been performed to generate desired high-pressure and high-temperature ambient conditions [15]. Premixed mixture of  $C_2H_2$ ,  $H_2$ ,  $O_2$  and  $N_2$  is first filled in the combustion vessel to the desired gas density. A pre-burn event of the mixture ignited by a spark inside the combustion vessel follows and raises the gas temperature to about 2000 K. Gas temperature decreases to the vessel temperature within about 5 seconds due to the rapid heat transfer. Fuel injection is triggered halfway of the cooling process when the bulk gas temperature reaches 900 K. With 15% oxygen level in the ambient gas, the injected diesel fuel auto ignites and generates complex turbulent flame. Detailed test conditions are listed in Table 1.

Parameter	Value
Amb. Density	25.4 kg/m <sup>3</sup>
Amb. Temp.	900 K
Amb. O <sub>2</sub>	15%
Nozzle Dia.	100 μm
Nozzle k-factor	1.5
Inj. Press.	70, 120, 180 MPa
Inj. Duration	~ 4 ms
Fuel	ULSD #2

Table 1. Test conditions

The combustion vessel features with a cubic-shaped chamber and three of the cubic walls are optically accessible as shown in Fig. 1.

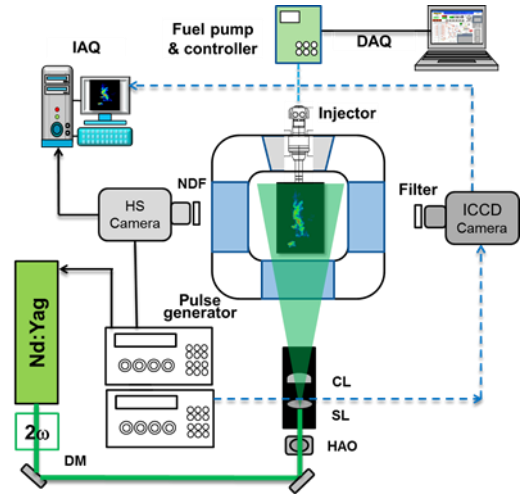


Fig. 1. Experimental setup for LII and flame luminosity.

A High-Speed (HS) camera (Photron FASTCAM SA1.1) and an Intensified CCD (ICCD) camera are placed perpendicular to the injector axis, taking the view through the side windows. Visible flame luminosity was captured by the HS camera with a neutral density filter (optical density 0.8) to avoid detector saturation. The HS camera is operated at 40,000 fps with 2.8 μs shutter time. On the opposite side, the ICCD camera was used to obtain the LII signal induced by an Nd:YAG laser sheet of 532 nm illuminating on the spray flame head. The laser energy fluence level is approximately 1 J/cm<sup>2</sup>, which is sufficient to make the LII signal independent of laser power [14]. A band-pass 400 nm filter (bandwidth FWHM 20 nm) was mounted to suppress flame luminosity. The gate time for ICCD camera was 300 ns. During the experiment, for all tested conditions, the HS camera starts to record the flame luminosity at the start of injection (SOI) for 5-ms duration while the laser is triggered 2.7ms after SOI and the ICCD camera captures the LII signal at that time instant.

### Image Analysis Methods

As the images to be correlated are obtained from two different cameras, it is necessary to perform an image adjustment to achieve pixel-to-pixel alignment. Based on the calibration image taken prior to the tests, the ICCD camera has a finer resolution (78.9 μm/pixel) than the HS camera (175.8 μm/pixel), and all images are resized to the ICCD image size and resolution. Image alignment was performed by flipping the HS image and matching the injector tip location. Pixels of zero intensity values are padded where necessary.

Sample raw images of LII and flame luminosity signals are shown in Fig. 2 for one test run at 120 MPa injection pressure, where the spray evolution is from right to left. Although band-pass filtered and extremely short exposed, signals captured by the ICCD camera does not reflect pure soot distribution within the plane of laser

sheet. A portion of flame luminosity would be detected on the detector as background interference. The *soot islands* are defined in Fig. 2 by setting the threshold at 10% of maximum signal intensity. Comparison and analysis will be focused on the signals from these soot islands of real LII.

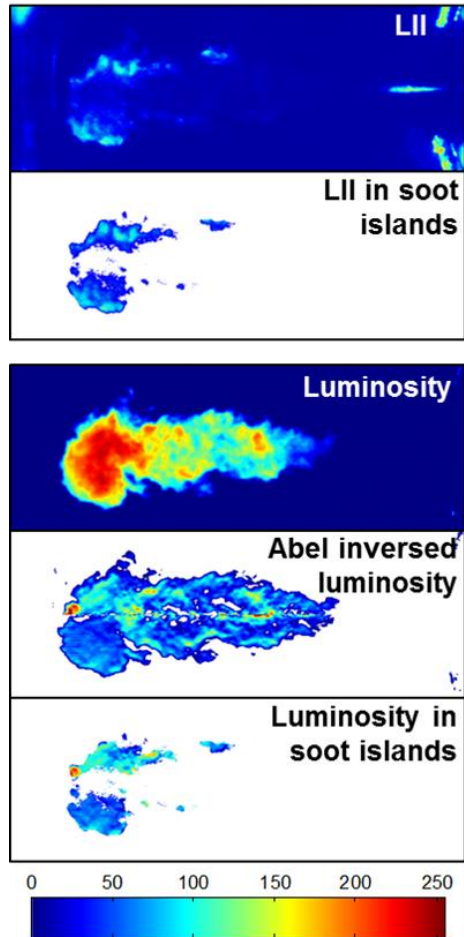


Fig. 2. Image processing procedure for 2D-based correlation. Top two figures are original and processed LII signals. Bottom three figures are original and processed luminosity.

Image correlation was performed between the LII image and the frame of HS image at 2.7 ms after SOI. Although both images show the soot field information at the same instant of a single injection event, an image conversion is necessary before obtaining the correlation. This is due to the characteristics of the imaging techniques. For the flame luminosity signal acquisition, as the camera is perpendicular to the jet axis, an integral of luminosity along line of sight was accumulated. Thus, the HS images illustrate the volumetric soot information (3D) with the burning jet's thickness taken into consideration. On the other hand, the LII signal is generated by a thin laser sheet and the signals captured by the ICCD camera are just from a thin plane within the flame region. In other words, the LII signals are 2D soot distribution information in the fuel jet's center plane. It is necessary to convert both images on a same display base (either 2D or 3D) for comparison. A common practice of

tomography techniques is the Abel inversion. The Abel inversion requires that the imaged object is axisymmetric, which would be a reasonable assumption for the injected fuel jet as it can be regarded as symmetric with respect to the injector axis.

### Image correlation based on 2D intensity

A first attempt here is to deconvolute the volumetric integrated luminosity signals to a 2D based image using the three-point Abel inversion suggested by Dasch [16]. A two-step image processing is adopted for tested conditions. Deconvolution of the flame luminosity with Abel algorithm is the first step. Although it is assumed that the resulting flame from the jet is axisymmetric, the presence of turbulence changes the local geometry and makes the projected flame non-symmetric with respect to the axial spray centerline. Modification to the Abel inversion was applied to have the deconvolution performed separately in top and bottom halves from the image. The *Abel inverted luminosity* image in Fig. 2 displays the deconvoluted 2D information from HS camera images. The second step is to focus the analysis within the identified soot islands so that the resulting 2D soot distributions obtained by both techniques share the exact same regions of interest. A direct pixel-to-pixel intensity correlation analysis can be carried out between the images named *LII in soot islands* and *luminosity in soot islands* in Fig. 2.

By listing the corresponding pixel-to-pixel intensities from both processed images, a scatter plot can be generated for correlation analysis as shown in Fig. 3. The correlation coefficient for these two sets of intensity numbers is approximately 0.06, which is very weak correlation. The same approach has been applied for all other test runs.

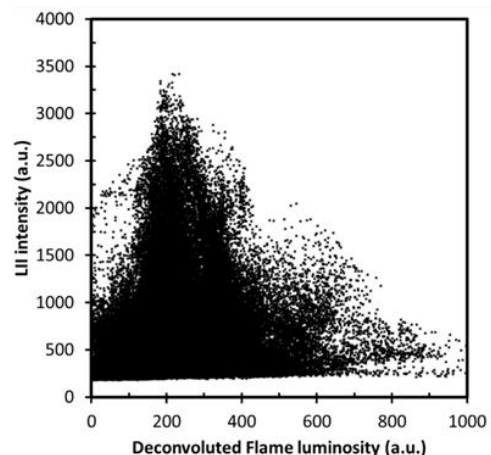


Fig. 3. 2D-based intensity correlation from Fig. 2.

### Image correlation based on 3D intensity

Instead of deconvoluting the volumetric information obtained in the luminosity images, a reverse procedure can be carried out. The 2D LII signal was processed through an integral transform to be comparable with the 3D luminosity signals. As for detailed procedure, the LII image was cropped within the soot islands first. Similar to the Abel inversion, the integration of LII intensities

was also done separately by the top and bottom halves. By revolving each half of images along the spray centerline by 180 degrees, the projected image intensities are summed up, resulting in the *Integrated LII* image in Fig. 4. The soot distribution region is defined by the boundary of the integrated LII signals and the original luminosity image is cropped into this region.

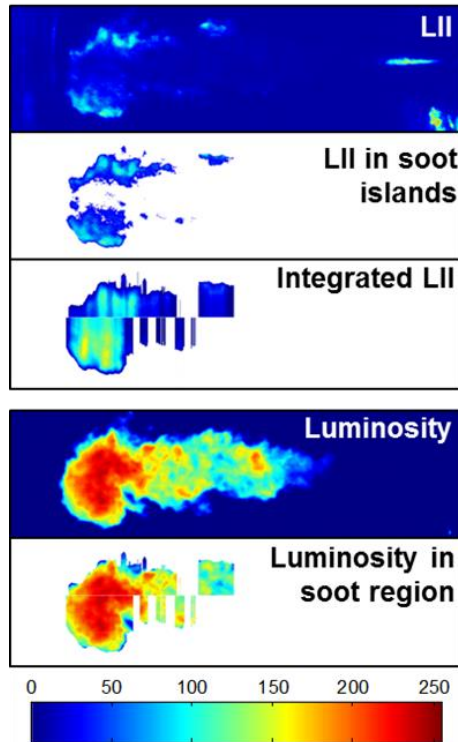


Fig. 4. Image processing procedure for 3D-based correlation. Top three figures are original and processed LII signals. Bottom two figures are original and processed luminosity.

Scatter plot of pixel-to-pixel intensity comparison for these 3D-based intensities is shown in Fig. 5. The correlation coefficient for the shown case (120 MPa injection pressure) is approximately 0.64.

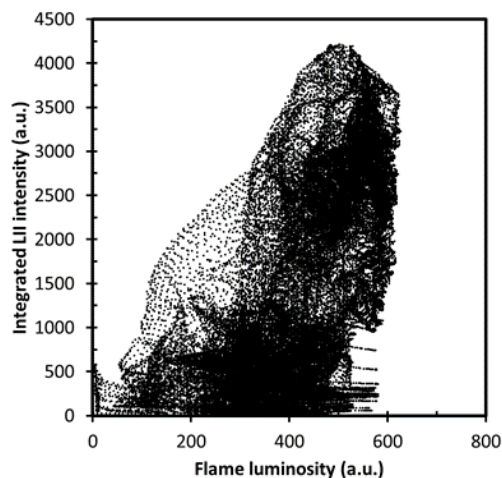


Fig. 5. 3D-based intensity correlation from Fig. 4.

A summary of correlation coefficients between the LII signals and flame luminosity is plotted in Fig. 6.

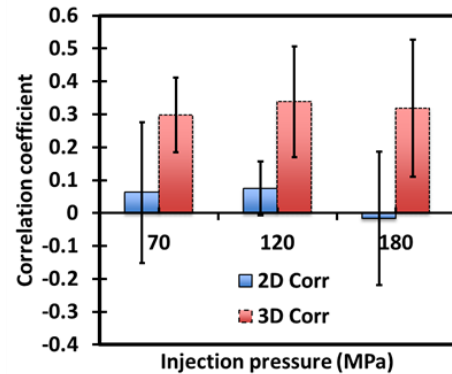


Fig. 6. Summary of intensity correlation coefficients for 2D and 3D analysis for the three injection pressures.

Note that the 70 MPa and 180 MPa injection pressure cases have 3 runs each while the 120 MPa injection pressure case has 8 runs. The correlation coefficient is a dimensionless parameter ranging from -1 to 1, where -1 indicates strong negative correlation, 1 indicates strong positive correlation and 0 indicates no correlation. The averaged correlation coefficients do not vary significantly with injection pressure for both 2D and 3D methods, however, a large variation of these coefficients is observed for almost all test conditions. For 2D correlation results, the average coefficients are below 0.1 while the 180 MPa case has a slightly negative value. The results of 2D image analysis suggest that the deconvoluted volumetric soot information can barely correlate with the instantaneous soot distribution in the center plane of the flame. Correlation coefficients obtained from 3D intensity analysis have average value of about 0.3, which shows a relatively weak positive correlation between the signals.

### Soot field structure

Original LII signal from Fig. 2 showed high intensity spots at the edge of the head vortex region of the burning jet, and the soot signal intensity is weaker in the core area. In addition, scattering and reflection of light from the liquid fuel and the combustion vessel walls are also captured as background noise. As for the luminosity image, a typical combusting jet structure of lifted flame can be recognized with a high-intensity head vortex. The conceptual model of diesel combustion proposed by Dec [1] states that high soot formation starts at the inner boundary of the diffusion flame within the head vortex and accumulates to higher level towards the core region of the flame during the quasi-steady combustion state. However, multiple results for low-sooting spray [6, 9], including the current research, observed only high soot area at the flame boundary with relatively low levels of soot in the core part. Fuel property may play an important role in this soot distribution scenario. When the soot generation is low, there is less chance for soot to accumulate into the flame core.



### Correlation results between two techniques

Results from the correlation analysis indicate that the correlation between the soot signals obtained through two different techniques do not match satisfactorily, even if the images were captured at the same time instant for identical combustion event. To address for such low correlation, differences between the two techniques and other possible reasons are explored and discussed in the following section.

Differences of LII and flame luminosity imaging exist in the viewing direction, the camera exposure time as well as the detected wavelength range. The two cameras in our setup share the same line of sight but are viewing the burning jet from opposite sides. Flame luminosity imaging captures the volumetric integration of light signal, which is not sensitive to the side selection; the LII imaging in this setup is viewing the center plane of the combusting spray, so the camera orientation should not affect signal structure either. Camera exposure time controls the number of photons impinging on the detector, thus varying the signal magnitude on the resulting image. Note that 300 ns and 2.8  $\mu$ s were used as exposure time for LII and flame luminosity, respectively. Although exposure times are quite different for both techniques, they are still short enough to be considered as instantaneous image with respect to the time scale of the burning spray, i.e., frozen flame. So the different exposure time is more likely to alter the image intensity levels. Correlation coefficient is mainly determined by the structure or distribution of soot signals rather than their magnitudes, thus exposure time can be eliminated as a major effect. Finally, the centerline wavelength for LII signal collection is at 400 nm while the luminosity imaging captures broadband signals that are mainly in visible range. The ICCD camera detector would respond uniformly to the narrow band signals, while the response curve varies with wavelength for broadband signals. It can be postulated that the HS camera detector distorts the luminosity distribution slightly due to its spectral response property, thus causing deviation on the image correlations.

Regarding the LII technique, it is usually necessary to account for the signal trapping influence. As the LII plane of interest is within the volumetric soot cloud, there exist soot particles along the line of sight between the laser sheet plane and the boundary of the flame. LII signals would be absorbed by these soot particles, leading to falsified information. Laser extinction measurement can be used to estimate the significance of this effect and provide correction to the resulting LII images [6]. Pickett et al. [6] performed signal trapping correction for LII measurement and found out it a minor influence on #2 diesel flame under ambient conditions similar to this study due to the low soot yield.

The presence of turbulence induced by momentum-driven combusting jet is believed to contribute to the low correlation results. Wide range of time and length scales can serve as the two major properties to characterize turbulence. As both techniques provide instantaneous images, the time scale of flame turbulence appears to be

longer than the exposure times and has minimum effect on the correlation results. On the other hand, turbulence with different length scales throughout the flame volume can highly alter the symmetry of the flame structure and soot distribution. The nearly non-correlated LII signal and Abel inverted luminosity can be an evidence of the destroyed symmetry of soot distribution. The non-symmetric details throughout the burning spray can be averaged out by the volumetric integration as the small length-scale fluctuation turns to sum up to relatively stable values at similar axial locations. This would also explain the increase in correlation coefficient when using 3D intensity comparison. However, given the still weak correlation for 3D signal analysis, it may suggest that turbulence of large length-scales that are comparable to the flame size also exists.

Lastly, we would like to address another difference between the natures of these soot detection techniques. As discussed in previous sections, the luminosity signal emitted from burning jet is the incandescence of soot particles within the diffusion flame boundary where temperature is high. The source of these light signals is the heated soot particles and there could exist soot particles that are not hot enough to glow at the same instantaneous time. Thus, the luminosity signals essentially show a portion of soot distribution whose particle temperatures are high. However, the LII provides an extra energy source that can raise the temperature of all soot within the laser plane to a saturation level. Ideally, the LII images can interpret a more complete picture of soot distribution regardless of the soot temperature within the flame region. If the number of soot particles within the combusting jet does not distribute evenly over the temperature span, the correlation between the two resulting images would also be skewed.

### Conclusions

Detailed quantitative correlation analysis of soot images obtained through LII and flame luminosity was performed in this study. The distribution characteristics of soot of diesel spray flame were discussed in detail from both spatial and temporal perspectives. It was found that the D#2 fuel is a low-soot fuel and the majority of soot forms at the inner boundary of diffusion flame in the head vortex of the combusting jet at tested conditions. In addition, a weak correlation was recognized between the 3D soot signals obtained through the two techniques. Turbulence with various length scales is considered as major cause for the low correlation. Moreover, the acquisition wavelength and temperature distribution of soot particles within the flame may also affect the correlation. Suggested future work is to conduct the same tests with band-pass filter for flame luminosity acquisition to remove the influence of camera spectral response. It will also be beneficial to perform multiple repeats to average out impact of turbulence.

## References

- [1] J.E. Dec, SAE Technical Paper 970873, (1997).
- [2] L.M. Pickett, D.L. Siebers, Proc. Combust. Inst., 29 (2002) 655-662.
- [3] M.P.B. Musculus, L.M. Pickett, Combust. Flame., 141 (2005) 371-391.
- [4] J.V. Pastor, J.M. García, J.M. Pastor, J.E. Buitrago, SAE Technical Paper 2005-24-012, (2005).
- [5] B.F. Kock, B. Tribalet, C. Schulz, P. Roth, Combust. Flame., 147 (2006) 79-92.
- [6] L.M. Pickett, D.L. Siebers, Int. J. Engine Res., 7 (2006) 103-130.
- [7] Y.-t. Han, K.-h. Lee, K.-d. Min, J. Mech. Sci. Technol., 23 (2009) 3114-3123.
- [8] S. Kook, L.M. Pickett, Proc. Combust. Inst., 33 (2011) 2911-2918.
- [9] E. Cenker, G. Bruneaux, L. Pickett, C. Schulz, SAE Int. J. Engines, 6 (2013) 352-365.
- [10] M. Kuribayashi, Y. Ishizuka, T. Aizawa, SAE Int. J. Fuels Lubr., 6 (2013) 641-650.
- [11] D. Siebers, B. Higgins, SAE Technical Paper 2001-01-0530, (2001).
- [12] D. Siebers, B. Higgins, L. Pickett, SaE technical Paper 2002-01-0890, (2002).
- [13] T. Kitamura, T. Ito, J. Senda, H. Fujimoto, Int. J. Engine Res., 3 (2002) 223-248.
- [14] C.R. Shaddix, K.C. Smyth, Combust. Flame., 107 (1996) 418-452.
- [15] A. Montanaro, L. Allocca, J. Johnson, S.-Y. Lee, J. Naber, A. Zhang, SAE Technical Paper 2013-24-0038, (2013).
- [16] C.J. Dasch, Appl. Opt., 31 (1992) 1146-1152.